6. House, H. O.; Gall, M.; Olmstead, H. D. *J. Org. Chem.* **1971**, *36*, 2361.
7. (a) Corey, E. J.; Boaz, N. W. *Tetrahedron Lett.* **1985**, *26*, 6019. (b) Alexakis, A.; Berlan, J.; Besace, Y. *Tetrahedron Lett.* **1986**, *27*, 1047. (c) Nakamura, E.; Matsuzawa, S.; Horiguchi, Y.; Kuwajima, I. *Tetrahedron Lett.* **1986**, *27*, 4029. (d) Johnson, C. R.; Marren, T. J. *Tetrahedron Lett.* **1987**, *28*, 27.
8. Caine, D. In *Carbon Carbon Bond Formation*; Augustine, R. L., Ed.; Marcel Dekker, New York, 1979; Vol 1, chapter 2.
9. Aluminum enolates: (a) Tsuda, T.; Satomi, H.; Hayashi, T.; Saegusa, T. *J. Org. Chem.* **1987**, *52*, 439. (b) Asaoka, M.; Hayashibe, S.; Sonoda, S.; Takei, H. *Tetrahedron Lett.* **1990**, *31*, 4761. Potassium enoxyborates: ref 5b. (c) Fortunato, J. M.; Ganem, B. *J. Org. Chem.* **1976**, *41*, 2194. Zincates. (d) Morita, Y.; Suzuki, M.; Noyori, R. *J. Org. Chem.* **1990**, *54*, 1787. (e) Takahashi, T.; Nakazawa, M.; Kanoh, M.; Yamamoto, K. *Tetrahedron Lett.* **1990**, *31*, 7349. (f) Lipshutz, B. H.; Wood, M. R. *J. Am. Chem. Soc.* **1994**, *116*, 11689. Quaternary ammonium enolates: ref 5c. (g) Smith III, A. B.; Mewshaw, R. *J. Org. Chem.* **1984**, *49*, 3685. For other references, see those cited in ref 5e and 8.
10. For a recent review, see: Chan, T.-H. In *Comprehensive Organic Synthesis*; Trost, B. M.; Fleming I., Ed.; Pergamon Press: Oxford, 1991; Vol 2, Chapter 2.3.
11. (a) Adlington, M. G.; Orfanopoulos, M.; Fry, J. L. *Tetrahedron Lett.* **1976**, 2955. (b) Varie, D. L. *Tetrahedron Lett.* **1990**, *31*, 7583.
12. For a review, see: Adlington, R. M.; Barrett, A. G. M. *Acc. Chem. Res.* **1983**, *16*, 55.
13. Scott, W. J.; Stille, J. K. *J. Am. Chem. Soc.* **1986**, *108*, 3033.
14. Brown, H. C.; Chen, J. C. *J. Org. Chem.* **1981**, *46*, 3978.
15. For a recent review, see: Burgess, K.; Ohlmeyer, M. J. *Chem. Rev.* **1991**, *91*, 1179.
16. For a review, see: Mancuso, A. J.; Swern, D. *Synthesis* **1981**, 165.
17. (a) Feutrill, G. I.; Mirrington, R. N. *Tetrahedron Lett.* **1970**, 1327. (b) Kende, A. S.; Rizzi, J. P. *Tetrahedron Lett.* **1981**, *22*, 1779.
18. McOmie, J. F. W.; West, D. E. *Org. Synth., Collect. Vol. V*, **1973**, 412.
19. Jung, M. E.; Lyster, M. A. *J. Org. Chem.* **1977**, *42*, 3761.
20. (a) Nishizawa, M.; Takenaka, H.; Nishide, H.; Hayashi, Y. *Tetrahedron Lett.* **1983**, *24*, 2581. (b) Nishizawa, M.; Morikuni, E.; Asoh, K.; Kan, Y.; Uenoyama, K.; Imagawa, H. *Synlett* **1995**, 169.
21. Baldwin, J. E. *J. C. S. Chem. Comm.* **1976**, 734.

Intramolecular Excimer Formation Processes of 1,3-Dipyrenylpropane in Silicate Sol-Gel

Misoo Kweon, Yun Hee Lee, Byung Tae Ahn, and Minyung Lee*

Department of Chemistry, Ewha Womans University, Seoul 120-750, Korea
Received October 11, 1995

The steady-state emission and fluorescence lifetimes of 1,3-dipyrenylpropane were measured in silicate sol-gel and xerogel matrices. In sol solution, the fluorescence emission spectra of monomer and excimer resemble those in hydrocarbon solvents. In gel and xerogel condition, however, the fluorescence spectra exhibit significant change, largely confirming the intramolecular motions in gel pores are influenced by microviscosity. The rate constants for intramolecular excimer formation were obtained from the measured fluorescence lifetimes and the rate processes for excimer forming in silicate sol-gel are described by a simple kinetic scheme.

Introduction

Organic molecules or polymers embedded in amorphous silica glass have drawn considerable attention during past few years as a new promising material.[1] They have a potential application in solar energy converter, solid-state laser dyes, and photonic devices. The organic/inorganic composites can not be prepared with high temperature glass melting technique, because the organic dopants decompose at much lower temperature than the melting point of inorganics. For this purpose, the sol-gel method, a room temperature processing technique, is usually employed to disperse guest organic molecules within the network of silica glass.[2]

To prepare organic/inorganic composite materials of high quality, it is necessary to understand the physical properties of organic dopants in microscopic sol-gel environment. The photophysical and photochemical properties of organic molecules in the inorganic matrices are expected to be quite different from those in organic solvents. For this purpose, many organic chromophores such as naphthalene, pyrene, and organic dyes have been studied in silica glass using absorption, fluorescence excitation and emission, and fluorescence anisotropy techniques.[3~6] The host matrix has been recently extended to other materials such as alumina, titania and zirconia.[7~11]

Pyrene has been widely used as a fluorescence probe to

investigate microenvironmental effects.[12] The pyrene forms excimer in highly concentrated solution, and these processes have been studied in solution,[13] high pressure fluid,[14] and sol-gel matrix[15] by several groups. Dipyrenylalkanes, Py-$(CH_2)_n$-Py, were also chosen for excimer formation processes. This dyad model compound forms excimer intramolecularly, so low concentration can be used for the photophysical study.[16,17] Therefore, it can serve as an ideal system to study dynamical behaviors of organic dopants in sol-gel-xerogel environment.

In this work, we used the 1,3-dypyrenylpropane (DPP) to study excimer formation during sol-gel processing. The fluorescence spectra of monomer and excimer were measured as a function of sol-gel aging time to extract information on environmental effects such as polarity and microviscosity. Fluorescence lifetimes were also measured to study intramolecular formation processes in sol-gel-xerogel transition. Rate constants for intramolecular formation were obtained from the measured experimental data. Comparing with solution phase results, dynamical aspects on intramolecular formation processes in silicate sol-gel are discussed in depth, based on a suitable kinetic scheme.

Experimental

1,3-bis(1-pyrenyl)propane used in this study was of the highest purity available. It was supplied by Molecular Probe Inc. Pyrene from Aldrich Co. was purified by recrystalization several times before use. Spectroscopic grade ethanol and tetraethylorthosilicate (TEOS) were used without further purification and the water was deionized and distilled. The initial solution was prepared from 18.5 mL of tetraethylorthosilicate, 9.0 mL of water and 23.5 mL of ethanol containing DPP. HCl was used for acid hydrolysis. The concentration of DPP in sol solution was maintained less than 1.0×10^{-5} M to prohibit intermolecular excimer formation. The mixture was put into a polystyrene cuvette, sealed with parafilm, and spectroscopic measurements were carried out as a function of aging time.

The fluorescence spectra and the emission lifetimes of the sample were measured at room temperature using the time-correlated single photon counting system from Edinburgh Analytical Instruments Co. The instrument response function of the system is about 1.0 ns. The excitation wavelength was 330 nm and the emission collection wavelength was 375 nm for monomer and 460 nm for excimer.

Results and Discussion

Steady-State Emission Spectra. Figure 1 shows the fluorescence emission spectra of DPP in TEOS solution, recorded as a function of aging time. The emission spectra were taken almost every day, but only five data are shown in the figure for clarity. The spectrum in sol solution is virtually the same as that in normal organic solvents: It shows structured emission bands in 360-430 nm due to the monomer emission and structureless broad emission band in 430-600 nm due to the excited dimer. As the aging proceeds, a dramatic change occurs around 43 days. The change is not only the decrease of excimer emission intensity, but also the decrease of the first vibronic band (377 nm) of the monomer emission.

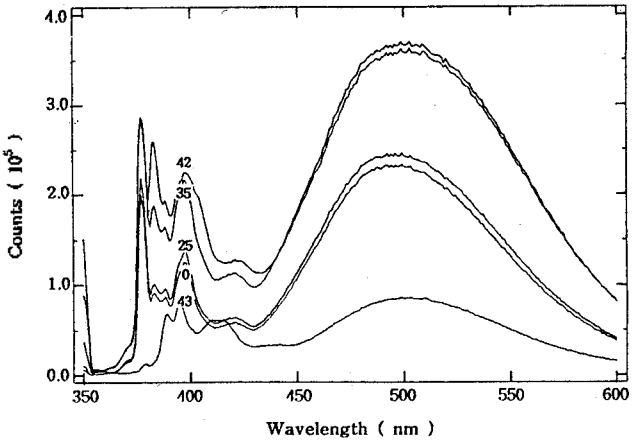

Figure 1. Fluorescence spectra of 1,3-Dipyrenylpropane in sol-gel system as a function of aging time (days).

Table 1. The ratio of $I_{excimer}/I_{monomer}$ and I_1/I_5 of 1,3-Dipyrenylpropanein silicate sol-to-gels

aging time (days)	$I_{excimer}/I_{monomer}$	I_1/I_5
0	5.33	1.58
30	5.33	1.58
35	5.32	1.58
40	4.68	1.33
42	3.02	1.25
43	2.50	1.07

Because there is some volume contraction as the matrices turn to the gel stage, the relative intensity ratio of the monomer and excimer emissions were chosen to compare each data set rather than the absolute intensity. Table 1 shows the ratio of the integrated intensity of monomer and excimer fluorescence, $I_{excimer}/I_{monomer}$, as a function of the aging time. The decrease of the intensity ratio upon gelation indicates that the excimer formation slows down, because the environment becomes more rigid. Considering fludity of the solution, the gelation point, a transition from sol to gel, is expected to occur around 25 days. The fact that the emission spectra do not change sharply in this region implies that the microenvironment for DPP is similar between sol and gel. In other words, there are sufficient solvents enclosing DPP even if gel is formed. If the matrix changes from gel to xerogel, most solvents are ejected from gel pores in this stage and pyrenes are in contact with the silica oxide network, which will affect the electronic (or vibronic) states of chromophores rather strongly. In this regard, the significant change on 43 days is attributable to gel to xerogel transition.

Pyrene momomer fluorescence usually shows five distinct peaks in the emission spectrum. The first vibronic band (I_1 band) occuring at 373 nm is forbidden in origin, but partially allowed in solution and enhanced by solvent polarity. The intensity ratio I_1/I_3 (or I_5) is indicative of microscopic polar enviornment of the flurescnece probe, which is known as the Ham effect.[12] The I_1 band of DPP in sol-gel solution is red-shifted to 377 nm. Up to the gelation point the ratio

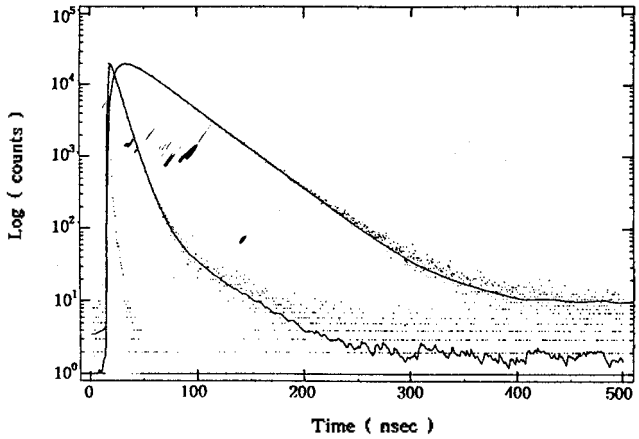

Figure 2. Typical intensity-time profiles of monomer and excimer of 1,3-dipyrenyl propane in sol solution. The excitation wavelength is 337 nm and fluorescence emission was collected at 373 nm for monomer and at 492 nm for excimer.

Table 2. The values of lifetime decay of 1,3-Dipyrenylpropane as a function of aging times

aging	monomer decay		excimer decay	
time (days)	relative amplitude	$\tau_{M,1}$ (ns)	relative amplitude	$\tau_{E,1}$, $\tau_{M,2}$, $\tau_{M,3}$ (ns)
0	0.99	7	−0.485	7
	0.01	38	0.346	39
			0.170	23
30	0.99	8	−0.485	7
	0.01	38	0.346	40
			0.170	23
35	0.99	8	−0.485	8
	0.01	40	0.346	40
			0.170	25
40	0.98	9	−0.434	8
	0.02	56	0.215	57
			0.350	37
42	0.98	11	−0.5	11
	0.02	78	0.170	72
			0.330	44
43	0.96	13	−0.458	12
	0.04	82	0.099	106
			0.443	48

exhibits a small change, but as long as the xerogel is formed, the I_1 band virtually diminishes after 45 days. The polarity experienced by DPP seems to decrease gradually as the gelation is processed further, and the first vibronic transition is almost forbidden, when the matrix becomes xerogel.

Lifetime Measurements and Kinetic Analysis. To understand excimer dynamics more fully, we carried out the time-resolved fluorescence study on DPP in TEOS solution. Figure 2 is the intensity-time decay profile of DPP in TEOS sol, and Table 2 contains all the data taken during the sol-gel-xerogel transition.

The monomer decay fits double exponential, while the excimer decay fits triple exponential:

$$I_M(t)=A_1 \exp(-t/\tau_{M,1})+A_2 \exp(-t/\tau_{M,2}) \quad (1)$$

$$I_E(t)=A_1' \exp(-t/\tau_{E,1})+A_2' \exp(-t/\tau_{E,2})+A_3' \exp(-t/\tau_{E,3}) \quad (2)$$

The amplitude sign of two terms in the monomer emission decay is positive, while that in the excimer decay consist of one negative (A_1') and two positives (A_2' and A_3'). The $\tau_{E,1}$, therefore, should be regarded as a rise time. In the excimer rise and decay, A_2+A_3 is equal to $-A_1$ within the experimental error.

Our data show that the two monomer components ($\tau_{M,1}$ and $\tau_{M,2}$) are the same as two excimer decay components ($\tau_{E,1}$ and $\tau_{E,2}$). Two monomer decay components indicate that there are two conformers which form excimer through two independent pathways.

Many kinetic schemes have been proposed for intramolecular excimer formation, and they are usually dependent upon model compounds. The excimer stabilization energy for pyrene dimer is *ca.* 7.8 kcal/mol which is more than ten times higher than thermal energy at room temperature, so there is little chance for which the excimer dissociates in the excited state during excimer lifetime. This greatly simplifies the kinetic schemes for pyrene intramolecular excimers. Ghiggino *et al.*[15] measured the fluorescence lifetime of DPP in hydrocarbon solvents and proposed the following scheme:

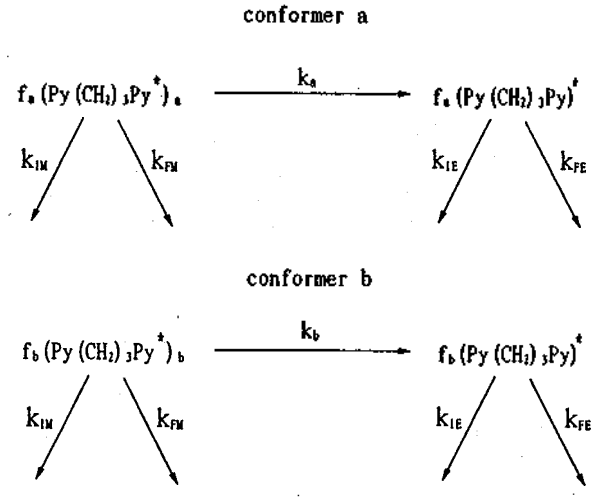

where f_a and f_b are the fraction of molecules in the ground state for conformers of type *a* and type *b*, respectively. k_a and k_b are the rate constants for excimer formation of conformer *a* and conformer *b*. k_{IM} (k_{IE}) and k_{FM} (k_{FE}) are nonradiative and ratiative decay constants for monomer (excimer). A kinetic analysis produces the following monomer and excimer fluorescence decay profiles accomodating all the parameters shown in the scheme.

$$I_M(t)=k_{FM}\,[f_a \exp(-t/\tau_{M,1})+f_b \exp(-t/\tau_{M,2})] \quad (3)$$

$$I_E(t)=k_{FE}\,[f_a \frac{k_a}{1/\tau_{E,3}-1/\tau_{E,1}} \exp(-t/\tau_{E,1})$$

Table 3. The values of rate constants of 1,3-Dipyrenylpropane as a function of aging times

aging time (days)	k_M (10^6 s^{-1})	k_E (10^6 s^{-1})	k_a (10^6 s^{-1})	k_b (10^6 s^{-1})
0	18	43	125	10
30	16	43	109	11
35	15	40	110	10
40	12	27	99	5
42	7	23	83	6
43	4	21	73	8

$$+f_b\frac{k_a}{1/\tau_{E,3}-1/\tau_{E,2}}\exp(-t/\tau_{E,2})$$
$$-\left\{f_a\frac{k_a}{1/\tau_{E,3}-1/\tau_{E,1}}+f_b\frac{k_b}{1/\tau_{E,3}-1/\tau_{E,2}}\right\}\exp(-t/\tau_{E,3})] \quad (4)$$

If we define k_M and k_D as $k_M=k_{IM}+k_{FM}$ and $k_E=k_{IE}+k_{FE}$, the following relations hold

$$1/\tau_{E,1}=k_a+k_M \quad (5)$$

$$1/\tau_{E,2}=k_b+k_M \quad (6)$$

$$1/\tau_{E,3}=k_E \quad (7)$$

$$f_a+f_b=1$$

Table 3 shows k_M, k_E, k_a, and k_b. k_M values which were obtained by measuring the fluorescence lifetimes of pyrene molecule at the each aging condition.

The experimental results for excimer decay gives the order of $1/\tau_{E,1}>1/\tau_{E,3}>1/\tau_{E,2}$, which makes the first term negative and the others positive in equation (4).

The relative population of type a to type b is more than 95% for all the aging condition. This indicates that type a configuration is much more energetically stable. Interestingly in hydrocarbon solvents, somewhat lower fraction (92%) has been observed. It is expected that the sol-gel solution stabilizes type a configuration more favorably compared with hydrocarbon solvents.

Intramolecular Excimer Formation Dynamics. In Table 3, the fluorescence decay constants of pyrene and pyrene excimer which were measured separately increase as a function of the aging time. This is just due to oxygen quenching, correlated with solvent viscosity. The rate constants show that the dynamic quenching process acts more efficiently for pyrene than for excimer. It has been known that the macroscopic viscosity change for sol to gel transition exceeds more than two orders of magnitudes.[6] The excimer formation process is a diffusional process, so the solvent viscosity affects the excimer formation from the monomer moieties. Our results show that the intramolecular formation dynamics of DPP entrapped in gel pores are governed by microscopic viscosity and polarity. The excimer formation rate constant k_a is about ten times faster than k_b. These values are in close agreement with the solution phase data.[15,16]

It is proposed that there exist two stable conformers in the ground state DPP in sol-gel-xerogel matrices. As shown in Figure 3, most conformers are in type a configuration

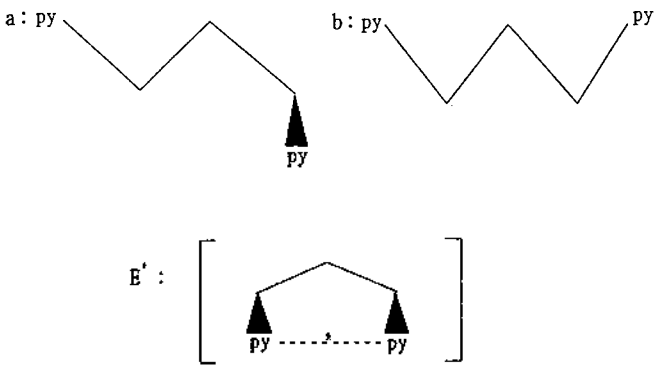

Figure 3. Schematics for type a and type b configuration of 1,3-dipyrenylpropane.

from which the intramolecular formation is more facile, possibly due to low activation energy, or shorter distance between two pyrene moieties in DPP. This is a different aspect compared to solution phase data. This may be explainable by considering the fact that DPP interaction with TEOS or silicate matrix favors the type a configuration.

In conclusion, we first studied the intramolecular excimer formation dynamics of dipyrenylpropane in silicate sol-gel solution. It is shown that the solvent polarity decreases as the aging proceeds, while the microviscosity in DPP experiences little change. There exist two stable conformers in the ground electronic state, which give distinct rate constants for excimer forming. The population of the confomer responsible for slow excimer formation is only a few percent. The excimer formation dynamics are simliar to the solution phase environment, except that the intramolecular formation processes in silicate matrix are significantly affected by microenvironment.

Acknowledgment. This work has been supported by the Basic Science Research Institute Program, Minstry of Education of Korea (BSRI-94-3427).

References

1. (a) Brinker, C. J.; Clark, D. E.; Ulrich, D. R. *Better Ceramics Through Chemistry III, MRS Symposium*; Reno, NV, 1988. (b) Reisfeld R.; Jorgensen, C. K. *Chemistry, Spectroscopy, and Applications of Sol-Gel glass*; Springer-Verlag: 1992. (c) Hench, L.; West, J. K. *Chemical Processing of Advanced Materials*, 1992.
2. Hench, L. L.; West, J. K. *Chem. Rev.* **1990**, *90*, 33.
3 Avnir, D.; Levy, D.; Reisfeld, R. *J. Phys. Chem.* **1984**, *88*, 5956.
4. Reisfeld, R.; Brusilovsky, D.; Eyal, M.; Miron, E.; Burstein, Z. *J. SPIE Proc.* 1182 230, 1989.
5. Yamanaka, T.; Takahashi, Y.; Kitamura, T.; Uchida, K. *Chem. Phys. Lett.* **1990**, *172*, 29.
6. Narang, U.; Wang, R.; Prasad, P. N.; Bright, F. V. *J. Phys. Chem.* **1994**, *98*, 17.
7. Pouxviel, J. C.; Dunn, B.; Zink, J. I. *J. Phys. Chem.* **1989**, *93*, 2134.
8. McKiernan, J.; Pouxviel, J. C.; Dunn, B.; Zink, J. I. *J. Phys. Chem.* **1989**, *93*, 2129.
9. McKiernan, J. M.; Yamanaka, S. A.; Dunn, B.; Zink, J.

I. J. Phys. Chem. **1990**, *94*, 5652.
10. Sanchez, C.; In M. J. Non-Cryst. Solids **1992**, *147&148*, 1.
11. Negishi, N.; Fujii, T.; Anpo, M. Langmuir **1993**, *9*, 3320.
12. See, for example, *Photochemistry in Organized and Constrained Media*; Ramamurthy V. Ed.; (1991) VCH Publishers, 1991.
13. Forster, T. Angew. Chem. **1969**, *8*, 333.
14. Hara, K.; Yano, H. J. Am. Chem. Soc. **1988**, *110*, 1911.
15. Snare, M. J.; Thistlethwaite, P. J.; Ghiggino, K. P. J. Phys. Chem. **1983**, *105*, 3328.
16. Reynders, P.; Kuhnle, W.; Zachariasse, K. A. J. Phys. Chem. **1990**, *94*, 4073.
17. Tsuchida, A.; Ikawa, T.; Tomie, T.; Yamamoto, M. J. Phys. Chem. **1995**, *99*, 8196.

Channel Electrode Voltammetric and *In Situ* Electrochemical ESR Studies of Comproportionation of Methyl Viologen in Acetonitrile

Chi-Woo Lee*†, John C. Eklund‡, Robert A. W. Dryfe‡, and Richard G. Compton‡

†*Department of Chemistry, College of Natural Sciences, Korea University, Jochiwon, Choongnam 339-700*
‡*Physical and Theoretical Chemistry Laboratory, Oxford University, South Parks Road, Oxford. OX1, United Kingdom*

Received October 14, 1995

Two redox processes of methyl viologen (+2/+, +/0) in acetonitrile were investigated by using channel electrode voltammetric and in situ electrochemical ESR methods. Two separated unequal plateau currents of the first (+2/+) and second (+/0) redox processes of the viologen were observed in the channel electrode voltammograms and showed a cube-root depedndence on the electrolyte flow rate, respectively. The simple Levich analysis resulted in two different diffusion coefficients of $D_{+2}=2.2\times10^{-5}$ cm²/s and $D_{+}=3.0\times10^{-5}$ cm²/s from the limiting currents. *In situ* electrochemical ESR studies were performed for the monocation radicals generated at the potentials of the two plateau currents in the electrolyte flow range $1.3\times10^{-1}\geq v_f \geq 2.7\times10^{-3}$ cm³/s. Backward implicit finite difference method was employed to simulate the electrochemical kinetic problem of two sequential electron transfers ($MV^{+2}+e \rightleftarrows MV^{+}$, $MV^{+}+e \rightleftarrows MV^{0}$) coupled with reversible comproportionation ($MV^{2+}+MV^{0} \underset{k_b}{\overset{k_f}{\rightleftarrows}} 2MV^{+}$). k_f was found to be greater than 10^6 M^{-1} s^{-1}.

Introduction

As part of continuing studies of understanding the thermodynamic aspects of and electrochemical kinetic effects by asymmetric surfactant viologens in organized molecular assemblies,[1,2] we have investigated the following two reductive electrochemical processes of viologens (V^{+2}) coupled with comproportionation in acetonitrile solutions by using channel electrodes.

$$V^{+2}+e^- \rightleftarrows V^{+} \qquad E^{o'}_{+2/+} \qquad (1)$$

$$V^{+}+e^- \rightleftarrows V^{0} \qquad E^{o'}_{+/0} \qquad (2)$$

$$V^{0}+V^{+2} \rightleftarrows 2V^{+} \qquad K \qquad (3)$$

Since the formal potentials of reactions (1) and (2), $E^{o'}_{+2/+}$ and $E^{o'}_{+/0}$, are separated by several tenths of a volt with $E^{o'}_{+2/+}$ less negative than $E^{o'}_{+/0}$, the thermodynamically spontaneous comproportionation between V^0 and V^{+2} produces the singly-reduced radical cation, which shows a strong ESR signal, at the potential corresponding to the overall $2e^-$ reduction of V^{+2}. Thus electrochemical method combined with ESR spectroscopy will be a method of choice to approach to solve the kinetic problem.

The channel electrode,[3] which utilizes the well-defined flow pattern inside the channel and the efficient numerical method of backward implicit finite difference (BIFD) for the geometry of channel flow cells, has been proved to be a useful hydrodynamic electrode for the mechanistic investigation of the electrode reactions which involve homogeneous chemical reactions. It consists of an electrode embedded in the wall of a rectangular duct through which electrolyte solution is flowed, as shown in Figure 1.

In situ electrochemical ESR method using the channel electrode has been successfully applied to tackel an irreversible comproportionation system by Compton.[4] The present work is to consider reversible comproportionation reaction by using channel electrode voltammetric and *in situ* electrochemical ESR methods experimentally and theoretically.

Comproportionation kinetics of methyl viologen has been studied by several different groups previously.[5~7] Our results agree with the reaction scheme (1)-(3) and large comproportionation rate constant (k_f) reported by others, and nonidentical plateau currents of the first and second redox processes and unequal diffusion coefficients of the viologen dication